

# Wind tunnel model studies to predict the action of wind on the projected 558 m Jakarta Tower

N. Isyumov<sup>†</sup>, P.C. Case<sup>‡</sup> and T.C.E. Ho<sup>‡†</sup>

*Boundary Layer Wind Tunnel Laboratory, The University of Western Ontario, London, Ontario, Canada*

R. Soegiarso<sup>‡</sup>

*PT Menara Jakarta, Jakarta, Indonesia*

**Abstract.** A study of wind effects was carried out at the Boundary Layer Wind Tunnel Laboratory (BLWTL) for the projected 558-m high free-standing telecommunication and observation tower for Jakarta, Indonesia. The objectives were to assist the designers with various aspects of wind action, including the overall structural loads and responses of the Tower shaft and the antenna superstructure, the local wind pressures on components of the exterior envelope, and winds in pedestrian areas. The designers of the Tower are the East China Architectural Design Institute (ECADI) and PT Menara Jakarta, Indonesia. Unfortunately, the project is halted due to the financial uncertainties in Indonesia. At the time of the stoppage, pile driving had been completed and slip forming of the concrete shaft of the Tower had begun. When completed, the Tower will exceed the height of the CN-Tower in Toronto, Canada by some 5 m.

**Key words:** Jakarta Tower; CN-Tower, aeroelastic model; pressure integration; Jakarta wind climate; aerodynamic response; vortex shedding; ECADI; wind tunnel; BLWTL; PT Menara Jakarta.

---

## 1. Introduction

The *Menara Jakarta* or the Jakarta Tower is designed to extend to about 558 m above ground. Structurally, it consists of 3 reinforced concrete tubes 13.2 m in diameter, arranged in plan in the form of an equilateral triangle with a centre to centre spacing of 32.9 m. These tubes are tied together at several levels and extend to a height of 323m above ground. This section of the Tower shaft is referred to as the triple tube. Beyond this a single central reinforced concrete tube continues to a height of 452 m. A steel antenna superstructure extends beyond this level to the full height of 558 m. Wind engineering studies for this structure included the following:

- 1) A statistical model of the Jakarta Wind Climate was developed.
- 2) Pressure model tests were made in turbulent boundary layer flows to provide information on local wind pressures on components of the exterior envelope and to determine the wind loads on the overall structure. The latter were obtained by spatially integrating simultaneously measured

---

<sup>†</sup> Research Director and Professor

<sup>‡</sup> Project Manager

<sup>‡†</sup> Research Director

instantaneous pressures at various levels along the Tower. A numerical model was then used to calculate the generalized wind forces for the first 9 modes of vibration of the Tower and to predict its wind-induced response using random vibration theory. This included the development of equivalent statically-acting wind loads which reflect the actual static and dynamic wind loading distributed over the height of the Tower. The equivalent statically-acting wind loads, determined so to reproduce the measured peak base bending moment, are used for the structural design and estimates of wind-induced motions and accelerations.

- 3) Confirmation of the overall wind forces were made using the pressure model mounted on a base balance. These tests provided a check on the spatial integration of the instantaneous pressures.
- 4) An aeroelastic model was designed and tested to confirm the findings of the pressure study and to provide detailed information on the response of the antenna superstructure, which could not be effectively studied with the pressure model. These tests ensured that no aeroelastic or motion-dependent effects were overlooked.
- 5) Winds at pedestrian level were studied in order to assure acceptable conditions.

This paper deals with the overall wind-induced structural loads and responses of the Tower; other information can be found elsewhere (Case *et al.* 1996). Even though Jakarta is not a high wind area, the predicted wind-induced overturning moments exceeded those due to seismic loads. The wind-induced drift and accelerations influenced the performance of the Tower and the habitability of the restaurant and other occupied levels. Finally, there was a design requirement to limit the wind-induced rotations of the antenna in order to maintain transmission quality.

None of these questions are particularly unusual and have been examined for many other tall structures; notably the 553 m high CN-Tower in Toronto, Ontario, which has also been studied at the BLWTL (Isyumov *et al.* 1984). What makes the findings of this study interesting, however, is that the Jakarta Tower, once constructed, will become the tallest free-standing structure in the world and that its wind engineering studies represent state-of-the-art technology, not available at the time of the CN-Tower tests.

## 2. Jakarta wind climate

Jakarta is situated at the periphery of two typhoon basins: the Western North Pacific typhoon basin and the Northwest Australian typhoon basin. Nevertheless, tropical storms of typhoon intensity rarely affect the region and non-typhoon winds govern design.

A mathematical wind climate model for the Jakarta area was assembled to place equal emphasis on all wind directions and to predict a mean hourly wind speed of 40 m/s at gradient height for a return period of 100 years. This “circular” wind climate model reflects the strength of winds established in other BLWTL wind tunnel studies for this region of the world, and includes a somewhat conservative expectation for wind speeds at Jakarta. The assumption that severe winds are equally likely from any direction is a relatively inconsequential one as the structure is nearly axi-symmetric.

Predictions of extreme mean hourly wind speeds for various return periods are presented in Fig. 1. The predicted mean hourly wind speed at gradient height is approximately 38 m/s for a return period of 50 years. The Indonesian Wind Code specifies a basic design mean hourly wind speed of 20 m/s at a height of 10 m for ‘land’ sites and 25 m/s for sites located along the ‘sea-shore’. These design values are shown in Fig. 1 as a range at surface (10 m) values and as extrapolated to gradient height. Estimates made by researchers at the Bandung Institute of Technology, corroborate these

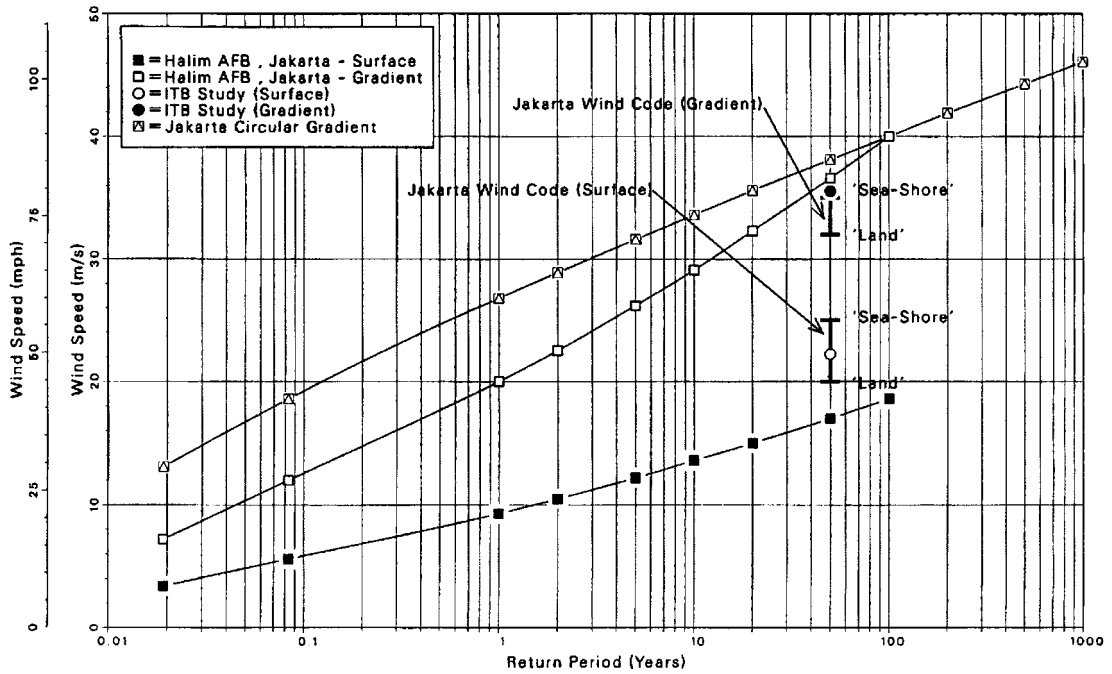


Fig. 1 Predicted extreme mean hourly wind speeds for various return periods at Jakarta, Indonesia

code values (see data denoted by 'ITB'). Predictions of surface and gradient wind speeds from data at the Halim Airforce Base are based on an analysis carried out at the BLWTL. The finally selected Jakarta Circular Gradient wind climate envelopes these estimates at the design return period of 100 years and intentionally includes some conservatism at lower return periods where the effects of thunderstorms may not have been fully captured in the data base.

### 3. Overview of wind tunnel tests

All wind tunnel model tests for the Tower were conducted at a geometric scale of 1:350. This scale was selected to achieve as large a model as possible without incurring excessive blockage maintaining model Reynolds Numbers ( $Re$ ) for all circular cross sections, except those in the antenna, to be in the  $3$  to  $4 \times 10^4$  range. Tests at  $Re$  values approaching and in the critical region are difficult to translate to full scale.

The simulation of natural wind at the project site was achieved with surface roughness along the wind tunnel floor, upstream of the model, and spires at the entrance to the working section of the wind tunnel. The mean and turbulence intensity profiles and spectra were in good agreement with ESDU 74031 data for open country and suburban terrains. The site of the Tower is well north of the built-up portion of Jakarta and towards the Java Sea.

A photograph of the pressure model of the Tower is shown in Fig. 2.



Fig. 2 Photograph of Menara Jakarta pressure model

## 4. Structural loads and responses from pressure measurements

### 4.1. Overview

Simultaneous measurements of the instantaneous pressures at various levels along the Tower were used to evaluate the generalized wind forces for the first nine modes of vibration. The modal displacements (mode shapes) and frequencies were provided by the East China Architectural Design Institute (ECADI). The first two modes were the fundamental sway modes in orthogonal  $x$  and  $y$  directions, each with period of 7.39 seconds. Modes 3 and 4 were fundamental antenna sway modes with little motion of the main shaft. Modes 5 and 6 and modes 8 and 9 were further pairs of  $x$  and  $y$  sway modes involving both antenna and shaft motions. Mode 7 was the fundamental torsional mode with an estimated period of 1.63 seconds.

The pressure tests were carried out at a mean wind speed of approximately 15 m/s in the free stream of the wind tunnel. The  $Re$  Number for the individual tubes of the triple tube portion of the Tower shaft were in the range of 3 to  $4 \times 10^4$ . This is a region where the aerodynamic characteristics of the model Tower were expected to be relatively invariant with  $Re$ . When converting to full scale, the along-wind forces were adjusted downward to allow for anticipated differences in model and prototype drag coefficients. Forces on sections consisting of a single cylinder were multiplied by 0.6. Forces on the triple tube portions were multiplied by 0.82, as it was argued that at model scale while the drag forces were somewhat conservative, the wider wakes result in a greater shielding of leeward portions. This reflected previous experience with a similar cross-section (Isyumov *et al.*

1984). No adjustment for  $Re$  differences was made for the across-wind response, which proved to be substantially lower than the drag response.

#### 4.2. Analysis procedure

Recorded time histories of simultaneous pressures at various levels along the tower were used to determine the instantaneous wind forces on the structure. This was done by assigning a surface area to each pressure tap and integrating the local forces at every instant of time over the exterior of the Tower. Forces in the  $x$ ,  $y$  and torsional directions were determined from the integration of the simultaneously acting pressures at all locations.

For a wind direction  $\alpha$  the contribution to the overall  $x$  and  $y$  forces and torque about the vertical axis are :

$$F_{xi}(\alpha, t) = p_i(\alpha, t) b_i h_i C_{xi} \quad (1)$$

$$F_{yi}(\alpha, t) = p_i(\alpha, t) b_i h_i C_{yi} \quad (2)$$

$$F_{\theta i}(\alpha, t) = F_{xi}(\alpha, t) arm_{xi} + F_{yi}(\alpha, t) arm_{yi} \quad (3)$$

where  $F_{xi}(\alpha, t)$  and  $F_{yi}(\alpha, t)$  are the forces in the  $x$  and  $y$  directions and  $F_{\theta i}(\alpha, t)$  is the contribution to the torque due to  $p_i(\alpha, t)$  acting at location  $i$ , for wind direction  $\alpha$  at time  $t$ ;  $b_i h_i$  represent the tributary area for location  $i$ ;  $C_{xi}$  and  $C_{yi}$  are the directional transformations based on the orientation of the tributary area;  $arm_{xi}$  and  $arm_{yi}$  represent the torsional arms of the  $x$  and  $y$  forces from the vertical axis.

Instantaneous base moments and torque are calculated as follows:

$$BM_x(\alpha, t) = \sum_{i=1, n} F_{xi}(\alpha, t) z_i \quad (4)$$

$$BM_y(\alpha, t) = \sum_{i=1, n} F_{yi}(\alpha, t) z_i \quad (5)$$

$$T(\alpha, t) = \sum_{i=1, n} F_{\theta i}(\alpha, t) \quad (6)$$

where  $z$  is the height above ground and the summation includes all locations on the exterior of the structure.

Bending moments, and torque at other heights along the structure and other quantities can be determined, using expressions similar to those of Eqs. (4)-(6).

The instantaneous value of the generalized force for mode  $j$  becomes:

$$F_j^*(\alpha, t) = \sum_{i=1, n} (F_{xi}(\alpha, t) \phi_{xji} + F_{yi}(\alpha, t) \phi_{yji} + F_{\theta i}(\alpha, t) \phi_{\theta ji}) \quad (7)$$

where  $\phi_{xji}$  is the  $x$ -direction modal displacement for mode  $j$  at location  $i$ , with corresponding definitions for  $\phi_{yji}$  and  $\phi_{\theta ji}$ .

The mean, the background RMS and spectra of the base moments, torque and the generalized forces for the first 9 modes of vibration were determined for all wind directions. The calculations of

the resonant dynamic response followed modal analysis procedures. With the power spectrum of the generalized force for mode  $j$  determined, the spectral density of the generalized coordinate for mode  $j$  becomes :

$$S_{\eta_j}(f) = \frac{1}{K_j^2} |H_j(f)|^2 S_{F_j^*}(f) \quad (8)$$

where  $S_{\eta_j}(f)$  and  $S_{F_j^*}(f)$  are respectively the spectral densities of the generalized coordinate  $\eta_j$  and its generalized force  $F_j^*$  at frequency  $f$ ;  $K_j$  is the generalized stiffness of mode  $j$  and  $|H_j(f)|$  is its mechanical admittance.

For lightly damped structures the variance of the resonant component of  $\eta_j$  can be written as :

$$\sigma_{\eta_{kj}}^2 \cong \frac{1}{K_j^2} \frac{\pi}{4\zeta_j} f_{o_j} S_{F_j^*}(f_{o_j}) \quad (9)$$

where  $\zeta_j$  is the effective damping ratio for mode  $j$ .

Eq. (9) can be used to estimate all other response quantities due to wind-induced resonant vibrations in the various modes of vibration. Following this approach, the peak value of the base bending moment due to wind forces in the  $x$ -direction for a particular wind speed and wind direction can be written as :

$$\hat{BM}_x = \overline{BM}_x + g \left( \sigma_{BM_{xB}}^2 + \sum_{j=1,9} \sigma_{BM_{xR_j}}^2 \right)^{1/2} \quad (10)$$

Where  $\overline{BM}_x$  is the mean value;  $\sigma_{BM_{xB}}$  is the RMS of the background or non-resonant component;  $\sigma_{BM_{xR_j}}$  is the RMS value of the  $x$ -component base bending moment due to the action of inertia forces due to resonant vibrations in mode  $j$ ; and  $g$  is a peak factor typically in the range of 3.5 to 4.0 for hourly peaks. Similar expressions can be written for other measures of the response.

The effective damping for mode  $j$  can be written as  $\zeta_j = \zeta_{sj} + \zeta_{aj}$ , where  $\zeta_{sj}$  and  $\zeta_{aj}$  are respectively the structural and aerodynamic components of the damping. In the analysis of the pressure data, it was assumed that  $\zeta_{aj} = 0$  and  $\zeta_{sj} = 0.02$  for all modes. A structural damping ratio of 0.02 is a commonly accepted nominal value for reinforced concrete structures. Subsequent aeroelastic studies provided information on  $\zeta_a$ .

### 4.3. Selected results

Fig. 3 summarizes the variation of the  $x$  and  $y$  base bending moments for different directions of the wind for a gradient wind speed of 40 m/s, which has a predicted return period of 100 years in Jakarta.

These plots show the composition of the structural wind loads on the Tower shaft. The curves denoted as mean represent the variation of the mean or time average value. The curves, denoted as mean + B.G. represent the combined effect of the mean and the background dynamic wind excitation. The curves denoted as mean + B.G. + mode 1 also include the contribution of inertia forces due to resonant vibrations in mode 1. Finally, the curve denoted as peak represents the entire response including resonant contributions from all modes of vibration. These responses have been assembled following Eq. (10). In the notation used, a positive  $x$ -moment is a moment due to wind-induced forces in the positive  $x$ -direction. From Fig. 3, it is apparent that the effects of drag or the along-wind forces dominate the overall wind forces acting on the Tower shaft. The gust effect factor,

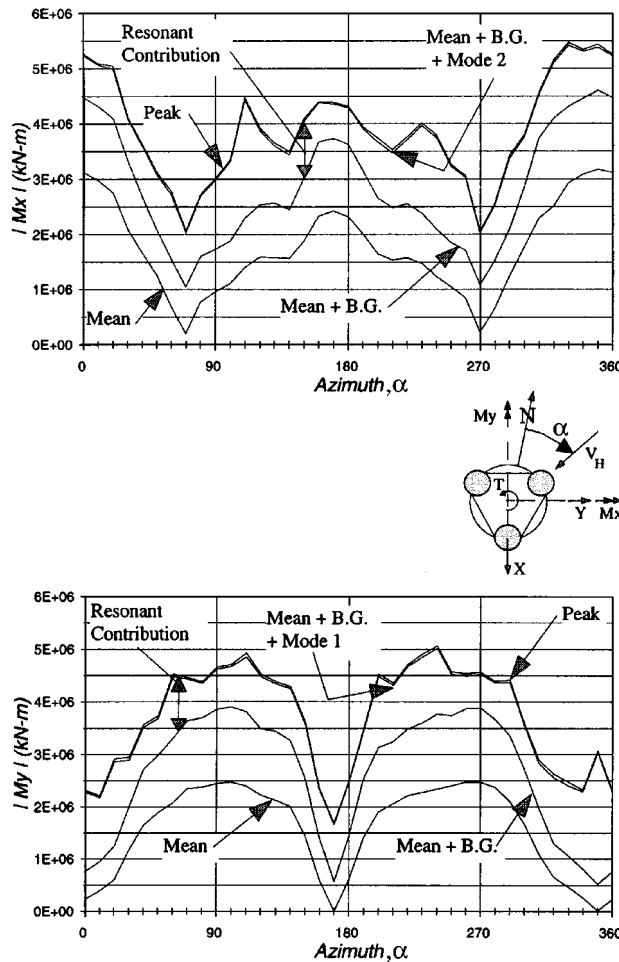


Fig. 3 Composition of the wind-induced base bending moments for  $v_g = 40$  m/s

defined as the peak base moment divided by the mean moment is in the range of 1.8 to 2. This is similar to the behaviour of the CN-Tower in Toronto (Isyumov *et al.* 1984). Furthermore, the non-resonant or background dynamic component is a major contributor to the total peak response. This is the case for both the drag direction, as seen from the  $x$ -moments for wind directions from approximately north and south and  $y$ -moments for approximately easterly or westerly winds, as well as other wind directions for which  $M_x$  or  $M_y$  represent the wind-induced across-wind moment, for example  $M_x$  for wind directions around  $90^\circ$  and  $270^\circ$ .

Similar information at a height of 347.5 m, which is above the top of the triple-tube portion of the Tower shaft is presented in Fig. 4. The composition and overall character of the peak response at this level is quite similar to that at the base, with marginally greater contributions from higher modes of vibration.

As expected, the torsional response of the Tower was relatively small. The 100-year return period peak deflection at the top of the Tower was predicted to be approximately 1.5 m. The 10-year return period accelerations at the restaurant, which is located at about 395 m, were predicted to be around

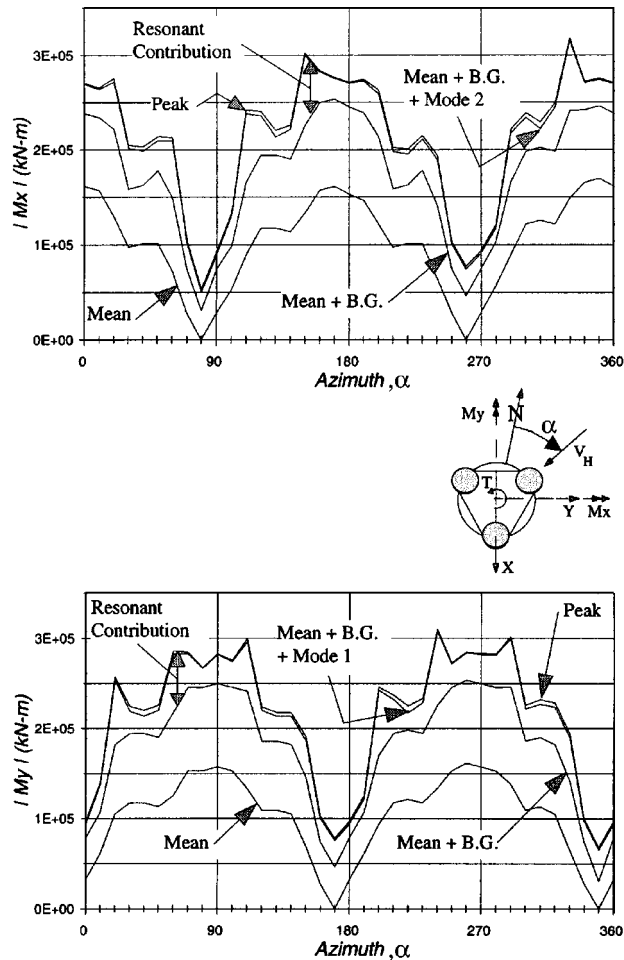


Fig. 4 Composition of the wind-induced bending moments above triple-tube at an elevation of 347.5 m above grade for  $\bar{V}_g = 40$  m/s

15 milli-g . This was judged acceptable based on criteria developed for tall buildings (Isyumov 1995).

## 5. Aeroelastic studies

### 5.1. Details of aeroelastic model

Aeroelastic model tests of the Tower were carried out at the same geometric scale as the pressure tests. Few surprises were anticipated for the Tower shaft. Based on the pressure tests, behaviour was dominated by wind-induced drag loads and additional resonance induced effects were limited to the fundamental sway modes with negligible contributions from higher modes of vibration. Nevertheless, this required confirmation. Furthermore, the aeroelastic tests were organized to provide additional information on the wind-induced performance of the antenna superstructure.

An equivalent aeroelastic model of the Tower was constructed. This was for both economic

reasons as well as concerns that a replica model would prove less accurate for higher modes of vibration, which were judged to be more dependent on the frame action of the triple-tube. In comparison, a replica aeroelastic model was constructed for the CN-Tower which has a gradually tapering post-tensioned concrete box section (Isyumov *et al.* 1984).

A schematic of the structural system used to represent the Tower is shown in Fig. 5. The equivalent structure follows the overall shape of the Tower with main vertical members arranged in the configuration of the triple-tube. Horizontal beam elements were used at the transfer levels to tie the individual tubes together. The structural system of the model became substantially simpler above the triple-tube and consisted of a central spine. The equivalent structural system was enclosed with a non-structural skin to obtain the correct external geometry. The exterior skin was discontinuous with definite horizontal and vertical cuts to avoid any contribution to the stiffness of the model.

The design of the equivalent structural system of the Tower proved to be a challenge. The

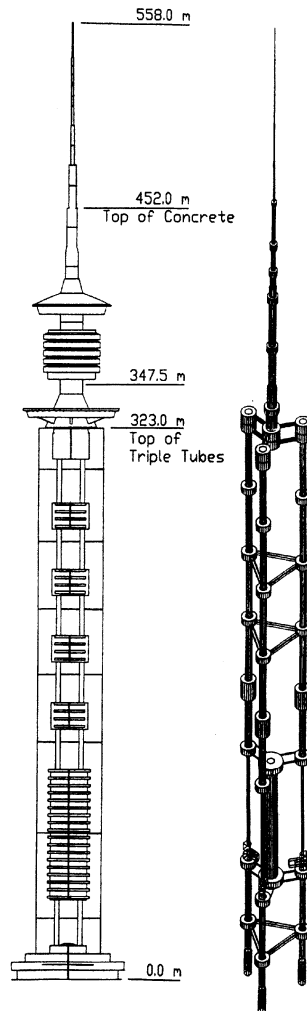


Fig. 5 Details of aeroelastic model

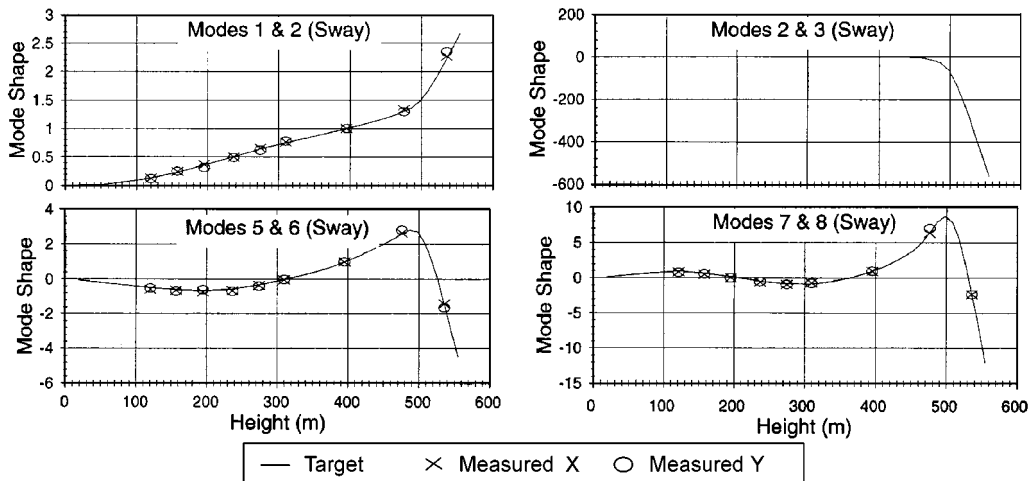


Fig. 6 Comparison of target and 1st eight as-built sway mode shapes

deformation of the Tower shaft due to horizontal loads proved to be a combination of shear and bending deformations and was therefore not easily scaled (Isyumov 1982, ASCE 1999). The design approach taken was to size the model structure so that the frequencies and the mode shapes of its first 8 sway modes of vibration matched the prototype. In this process, the mass and mass distribution of the model structure, including its various non-structural elements, was scaled to ensure similarity of the generalized masses. The fundamental torsional mode, which was found to be mode 7, was not modeled as torsional loads and responses were found to be minimal and were not simulated. As a result, modes 7 and 8 of the aeroelastic model simulated modes 8 and 9 of the prototype. Plots of the as-built and target mode shapes for the first 8 sway modes of vibration are summarized in Fig. 6. The as-built mode shapes were obtained by measurement using accelerometers. Corrections for the mass of the accelerometers were made. Agreement was excellent. The aeroelastic model was mounted on a stiff base balance to permit direct measurements of the base moments, including the effects of external forces and the additional inertia forces due to resonant vibrations. Measurements of  $x$  and  $y$  bending moments were also made at the base of the antenna (452 m in full-scale). Accelerations in the  $x$  and  $y$  directions were measured at restaurant level (395 m full-scale).

The damping of the aeroelastic model was determined to be approximately 1.75% for the fundamental modes 1 and 2 and in the range of 0.8 to 1% for modes 3 to 8.

## 5.2. Aeroelastic response

A comparison of  $x$  and  $y$  base bending moments obtained from the pressure integration and from the aeroelastic study are summarized in Fig. 7. These data include the external wind forces as well as the additional inertia forces due to wind-induced resonant vibrations. The data from the pressure integrations correspond to those already shown for a full-scale gradient wind speed of 40 m/s in Fig. 3. Only the mean and the peak values are given as it is relatively difficult to separate the aeroelastic data into their background and resonant dynamic components. In these comparisons, the resonant parts of the pressure data have been adjusted to a 1.75% fundamental mode damping ratio of the aeroelastic model. The drag components of the aeroelastic model response have been adjusted for

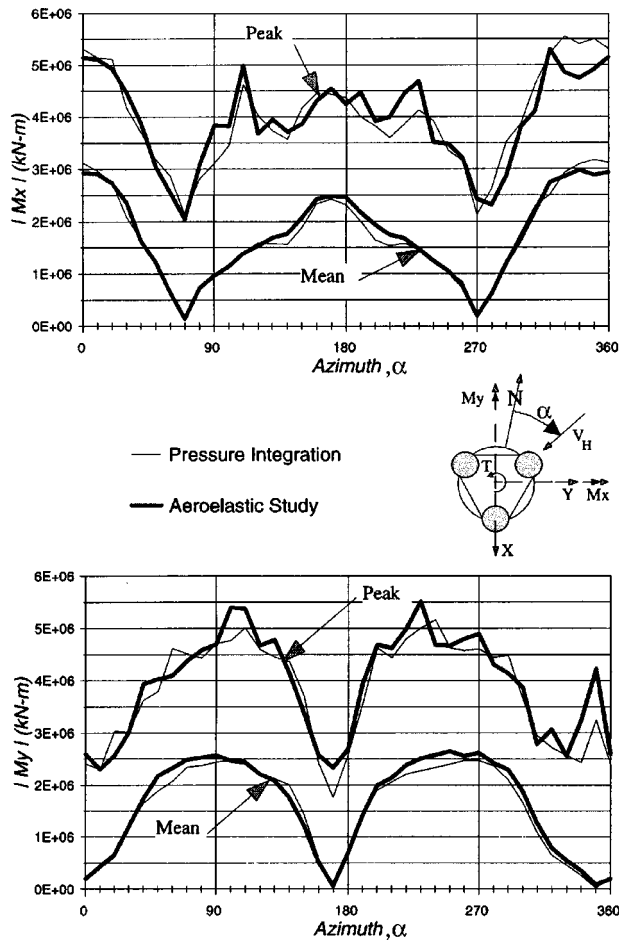


Fig. 7 Comparison of base bending moment obtained from the aeroelastic and pressure studies,  $\bar{V}_g = 40$  m/s

anticipated *Re* effects, following the same procedures as used for the pressure test data.

The agreement is generally good. Nevertheless, the dynamic across-wind response can be seen to be somewhat greater for some wind directions, particularly for  $\alpha = 350^\circ$ , which corresponds to a wind from project north and along a line of symmetry of the Tower shaft. This is the most open wind direction with the upstream fetch towards the Java Sea. Some increases can also be seen for wind directions of  $110^\circ$  and  $230^\circ$  which represent similar lines of symmetry. While the maximum response continues to be dominated by the drag loads which contain substantial mean and background components, the dynamic across-wind response is not negligible, particularly when considering load cases which include the combined action of *x* and *y* forces.

Inspection of Fig. 7 reveals that at an azimuth of  $350^\circ$ , for which the approach wind is along a line of symmetry of the Tower, that there are differences in the across-wind dynamic responses predicted by the aeroelastic and pressure studies. This is further apparent in Fig. 8 which shows RMS Base Moment data for a range of wind speed and for a structural damping of  $\zeta_s = 0.0175$  at the  $350^\circ$  azimuth. The aeroelastic model data capture all aspects of wind action, including any aeroelastic feed-back. The predictions from the pressure study method assume quasi-static aerodynamics

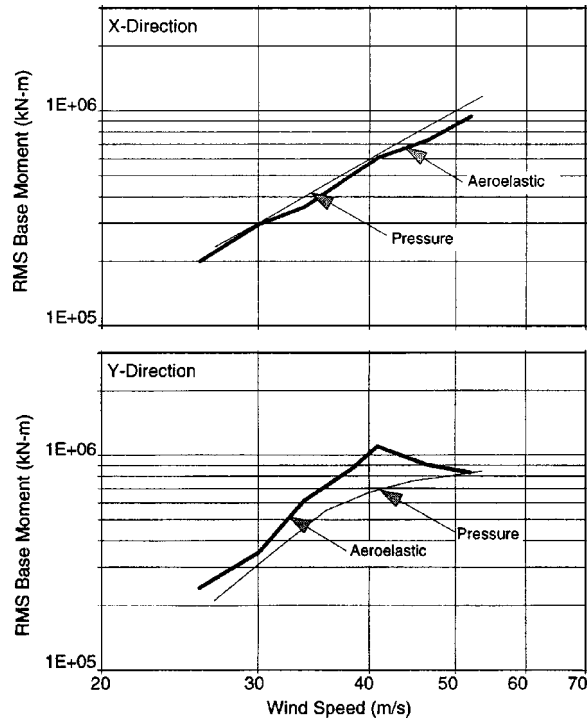


Fig. 8 RMS base moments for the 558 m Jakarta Tower predicted from the aeroelastic and pressure studies,  $\bar{V}_g = 40$  m/s,  $\zeta_s = 0.0175$ ,  $\alpha = 350^\circ$

and are based on the assumption that  $\zeta_a = 0$ . The dynamic response in the  $x$ -direction is due to drag forces and tends to be slightly overestimated, in comparison with the directly measured aeroelastic response. This is in part explained with the expectation that  $\zeta_a > 0$  for the drag direction.

The dynamic response in the  $y$ -direction is primarily due to vortex shedding induced vibrations in the fundamental  $y$  sway mode. The excitation is mainly from the shaft with a Strouhal Number of  $St \approx 0.16$ . Attempts to estimate  $\zeta_a$  from the spectra of the aeroelastic response proved somewhat inconclusive. This is not surprising as the damping is difficult to measure as a high frequency resolution is required. Invariably, all spectral techniques result in overestimates of the damping. The  $\zeta_a$  was estimated from the difference between the total damping, which is obtained from the spectral analysis of the response, and the structural damping which is obtained from free-vibration decay traces of the model with no wind (namely  $\zeta_a = \zeta_{total} - \zeta_s$ ). An overestimate of  $\zeta_{total}$  unfortunately underestimates negative values of  $\zeta_a$ .

Fig. 8 clearly demonstrates that the across-wind response can be underestimated without aeroelastic model tests unless special measures are taken to allow for the effects of possible aeroelastic feedbacks. Assuming  $\zeta_a \approx -0.01$  as one approaches a wind speed of about 40 m/s results in an improved agreement with the aeroelastic data in Fig. 8.

Fig. 9 shows power spectra of the  $x$  and  $y$  moments at the Tower base and at the base of the antenna for a wind direction of  $350^\circ$  and a full-scale gradient wind speed of 40 m/s. The resonant  $y$  response is seen to be primarily due to wind-induced across-wind vibrations in the fundamental mode of the Tower. The spectral distribution, which shows the contribution of particular modes of

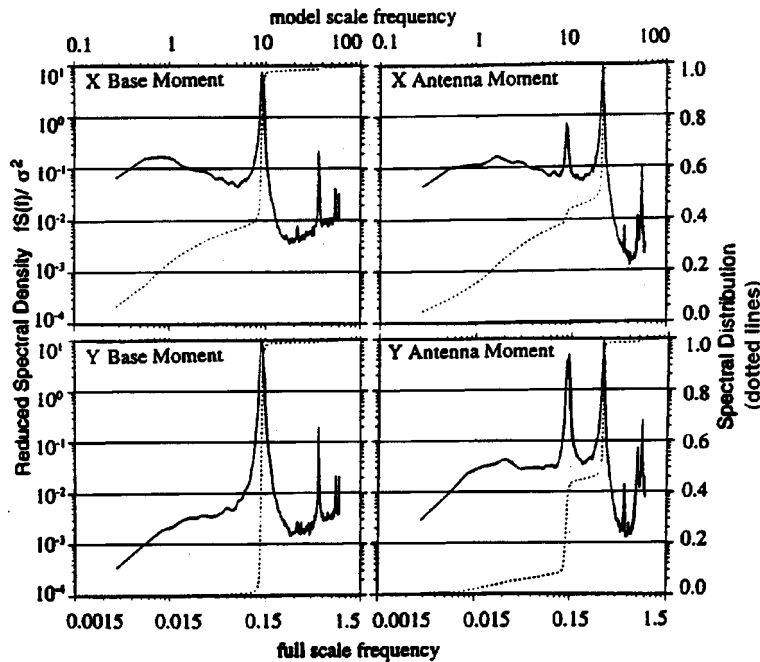


Fig. 9 Power spectra of tower and antenna base bending moments for  $\alpha = 350^\circ$ ,  $\bar{V}_g = 40$  m/s

vibration to the total variance, is indicated by the dotted lines. Examining the variation of the RMS y moment, there is a distinct peak at a full-scale gradient wind speed of 40 m/s confirming that the across-wind response is due to vortex shedding from the triple-tube shaft of the Tower. Based on the gross across-wind dimension of the triple-tube ( $D_{effective} = 32.9 + 13.2 = 46.1$  m in full scale), the Strouhal Number is  $St \approx 0.16$ . The aerodynamic damping for the across-wind response was found to be small. The spectra provided for the antenna moment are for the same wind speed and wind direction. The vortex shedding induced across-wind response in the fundamental mode of the Tower can be seen from the y bending moment spectrum. A substantial part of both the drag and along-wind dynamic response is seen to come from wind-induced vibrations in the third mode (second y sway mode).

Fig. 10 shows the envelope of the simultaneous x and y response of the Tower for several wind directions and a prototype gradient wind speed of 40 m/s. The response for the wind direction of  $350^\circ$  is seen to consist of mean and fluctuating components in the drag direction and simultaneous uncorrelated across-wind y direction response attributed to vortex shedding. The maximum response is still in the x direction due to the combined action of static and dynamic wind forces. Nevertheless, the across-wind response is clearly significant. The direction of the mean wind is shown in each of these figures. It is clear that in all situations the response of the Tower consists of drag and lift rather than x and y forces and motions. This is not surprising as the stiffness of the Tower shaft is essentially axi-symmetric. Furthermore, the orientation of the time averaged envelopes of the response indicates that the drag and across-wind forces are uncorrelated (the axes of the elliptical patches of the response are perpendicular and parallel to the wind vector).

The simultaneous responses of the x and y antenna moments indicate that the antenna response is drag-dominated. No unusual vortex shedding excitation was observed in any of the modes of vibration in the range of wind speeds considered to be of practical interest.

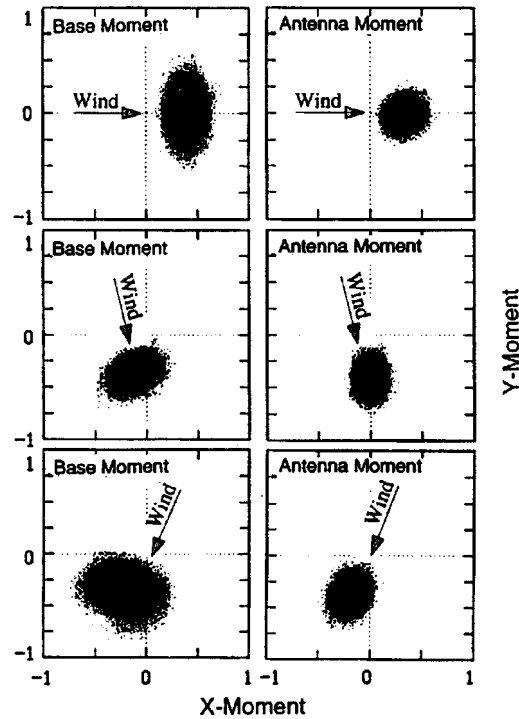


Fig. 10 Envelope of simultaneous  $x$ - and  $y$ -direction bending moments at tower and antenna base ( $x$  and  $y$  units plotted to same scale)

Wind-induced movements of the antenna are shown in Fig. 11. These are peak wind-induced deflections and slopes in the  $x$  and  $y$  directions for  $\alpha = 350^\circ$  and  $\bar{V}_g = 35$  m/s. The slope or rotation of the antenna in the  $x$  direction is  $\theta_x(z) = \{dx/dz\}_z$ , obtained by the differentiation of the  $x$  deformation along the length of the antenna denoted by  $z$ . The deflections represent the combined effects of all participating modes of vibration. These were evaluated by relating the deflection at any location along the antenna in a particular mode of vibration, to the antenna base bending moment due to the inertia forces in that mode. The participation of the various modes was obtained from the relative contributions of their power spectral peaks to the total variance of the antenna base moment. The static component of the deflection was assumed to have a shape corresponding to that of the deflection in the fundamental mode. As a result, the dynamic parts of the deflections and slopes are direct estimates from the results of the aeroelastic study, while the static components contain some approximation.

The data are presented for  $\bar{V}_g = 35$  m/s, which has a return period of 15 years, see Fig. 1, and therefore are more indicative of typical wind-induced responses. Examining both the deflections and the slopes, it becomes apparent that the response of the antenna is dominated by wind-induced drag forces. For  $\alpha = 350^\circ$ , the approach wind is in the  $x$  direction. The across-wind or  $y$  direction response in comparison is substantially lower. Not until  $\bar{V}_g = 40$  m/s, which corresponds to the 100-year return period design speed, does vortex shedding substantially influence to the behaviour of the tower shaft and the antenna.

While the gust effect factor for base overturning moments was found to be less than 2, the wind-induced dynamic response of the Tower becomes more significant higher up along the Tower. This

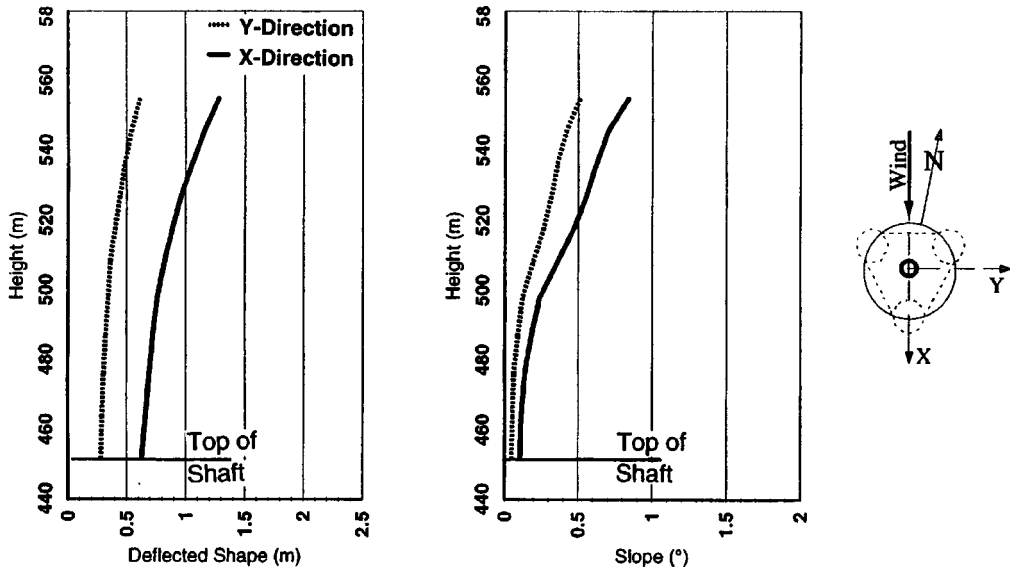


Fig. 11 Peak wind-induced deflections and slopes of antenna for  $\alpha = 350^\circ$  and  $\bar{V}_g = 35$  m/s

is apparent from the deflections and slopes near the top of the structure. The gust effect factor, defined as the peak value divided by the mean value, is approximately 2.7 and 3.7 respectively for deflections and slopes in the  $x$  direction at the top of the antenna. This is consistent with expected behaviour. Finally, the dynamic component of the wind-induced slope of the antenna both in the  $x$  and  $y$  directions is within the suggested limit of  $0.5^\circ$  considered desirable to assure broadcast quality.

## 6. Conclusions

This paper has described wind engineering studies for the projected 558 m high Jakarta Tower in Jakarta, Indonesia. The emphasis of the presented material has been on the wind-induced overall structural loads and responses of the Tower. Information on structural loads was developed from the spatial integration of simultaneously measured point pressures on exterior surfaces of the Tower. This is a powerful technique for assembling the structural loads, including the generalized wind forces for various modes of vibration. The response of the Tower is then obtained using modal analysis and random vibration theory. Using this technique, the wind-induced drag or along-wind forces were predicted to dominate the wind-induced loads and responses of the Tower. The static and the background or non-resonant dynamic response were found to be major contributors to the peak with resonant vibrations primarily confined to the fundamental modes of the Tower.

Aeroelastic studies were carried out to confirm the findings of the pressure study, to examine possible additional motion dependent or aeroelastic effects. These tests also provided more detailed information on the wind-induced performance of the steel antenna superstructure. An equivalent aeroelastic model of the Tower was designed, and constructed to simulate the dynamic properties of the prototype structure in its first 8 sway modes of vibration. Wind-induced torsional effects were small and the torsional dynamic characteristics of the Tower were therefore not simulated.

The aeroelastic model generally confirmed the importance of the drag or along-wind excitation of the structure. The aeroelastic studies showed that the dynamic response of the Tower was organized

by the excitation to be in the drag and lift rather than the  $x$  and  $y$  directions. The vortex shedding induced across-wind excitations for the azimuth of  $350^\circ$ , which corresponds to a line of symmetry of the Tower with 2 of the 3 component tubes of the triple-tube shaft facing the wind. The Strouhal number based on the total shaft width was  $St \approx 0.16$ . An aerodynamic damping of  $\zeta_a \approx -0.01$  is estimated for this direction at the design wind speed of 40 m/s at gradient height.

It was found that the drag or along-wind forces dominated the wind-induced response of the antenna superstructure. No significant vortex shedding excitation was found for wind speeds of practical interest.

In closing, it is interesting to make some overall comparisons. Table 1 summarizes the maximum peak base bending moments predicted for a return period of 100 years for a nominal structural damping of 1.5 to 2%. Differences in this range will have only minimal effects on the peak values which are to a large degree influenced by the static and background dynamic components of the wind loads. Included are predictions obtained from the integration of simultaneous pressures and aeroelastic tests. Also included are estimates made by ECADI, designers of the Tower, using procedures of the Chinese Code. These are remarkably close to the results of the wind tunnel study. This is not surprising as procedures for estimating the wind-induced drag response are now well established. Also included are comparisons with the wind-induced response of the CN-Tower in Toronto, Ontario, Canada (Isyumov *et al.* 1984). Two designs for the CN-Tower were studied. The initial design had a triple-tube shaft not dissimilar to that of the Jakarta Tower. The final design was a continuously tapered post-tension concrete box section. The CN-Tower data have been adjusted to the Jakarta wind climate to permit direct comparisons. Both the initial and final design of the CN-Tower have a much "slimmer" silhouette with less sail area near the top of the Tower. This is reflected in the peak base overturning moments.

Table 1 Comparisons of 100-year peak overturning moments ( $\bar{V}_g$  (100 yr) = 40 m/s)

	Peak base moment (kN.m) $10^6$	
	X-Dir	Y-Dir
Jakarta Tower (558 m)		
· BLWTL pressure studies	5.1	4.5
· BLWTL aeroelastic model	4.6	4.6
· Predictions by ECADI (based on Chinese Code)	5.0	4.4
CN-Tower (553 m) Jakarta Wind Climate		
· Initial triple-tube design (not built)	3.8	3.8
· Final "built design"	2.7	2.7

## References

- American Society of Civil Engineers (ASCE) (1999), Manual of practice No. 67 Wind tunnel model testing of buildings and structures.
- Case, P.C., Ho, T.C.E., Isyumov, N. and Mikiutiuk, M. (1996), "Wind engineering studies for the Menara Jakarta", Jakarta, Indonesia, The University of Western Ontario Report BLWT-SS25-1996, London, Ontario, Canada.
- Isyumov, N., Davenport, A.G. and Monbaliu, J. (1984), "CN-Tower, Toronto: Model and full-scale response to wind", *12<sup>th</sup> Congress IABSE*, Vancouver, B.C., Canada, September.
- Isyumov, N. (1982), "The aeroelastic modeling of tall buildings", *Wind Tunnel Modeling for Civil Engineering Applications*, Cambridge University Press.
- Isyumov, N. (1995), "Motion Perception, Tolerance and Mitigation", *Proc. 5<sup>th</sup> World Congress of CTBUH*, Amsterdam Netherlands.